THE JOURNAL OF PHYSICAL CHEMISTRY B

Article

pubs.acs.org/JPCB

Interactions of Histone Acetyltransferase p300 with the Nuclear Proteins Histone and HMGB1, As Revealed by Single Molecule Atomic Force Spectroscopy

S. Banerjee, T. Rakshit,[‡] S. Sett, and R. Mukhopadhyay*

Department of Biological Chemistry, Indian Association for the Cultivation of Science, Jadavpur, Kolkata 700 032, India

Supporting Information

ABSTRACT: One of the important properties of the transcriptional coactivator p300 is histone acetyltransferase (HAT) activity that enables p300 to influence chromatin action via histone modulation. p300 can exert its HAT action upon the other nuclear proteins too—one notable example being the transcription-factor-like protein HMGB1, which functions also as a cytokine, and whose accumulation in the cytoplasm, as a response to tissue damage, is triggered by its acetylation. Hitherto, no information on the structure and stability of the complexes between full-length p300 (p300FL) (300 kDa) and the histone/HMGB1 proteins are available, probably due to the presence of unstructured regions within p300FL that makes it difficult to be crystallized. Herein, we have adopted the high-resolution atomic force microscopy (AFM) approach, which allows molecularly resolved three-dimensional contour mapping of a protein molecule of any size and structure. From the off-rate and activation barrier values, obtained using single molecule dynamic force spectroscopy, the biochemical proposition of preferential binding of p300FL to histone H3, compared to the octameric histone, can be validated. Importantly, from the energy landscape of the dissociation events, a model for the p300−histone and the p300−HMGB1 dynamic complexes that HAT forms, can be proposed. The lower unbinding forces of the complexes observed in acetylating conditions, compared to those observed in non-acetylating conditions, indicate that upon acetylation, p300 tends to weakly associate, probably as an outcome of charge alterations on the histone/HMGB1 surface and/or acetylation-induced conformational changes. To our knowledge, for the first time, a single molecule level treatment of the interactions of HAT, where the full-length protein is considered, is being reported.

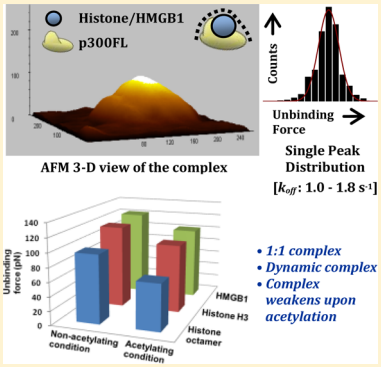

INTRODUCTION

The p300, an important transcriptional coactivator, is endowed with histone acetyltransferase activity (HAT),[1,2] which promotes histone acetylation, an event considered to be one of the key mechanisms behind access of a transcription factor to the firmly packed DNA in chromatin, during eukaryotic transcription. The p300 is thought to acetylate particularly the N-terminal lysine residues of histone H3, as well as histones H2A, H2B, and H4, with specific preference for H3K14,[3] H3K18,[4] and H3K56.[5] One consequence of acetylation of the histone tails is thought to be reduction of the net positive charge of histone,[6,7] leading to relaxation of its interaction with the negatively charged DNA, aiding access of transcription factors to the respective target gene sequences. Understanding the nature of interactions between p300 and histone proteins, and its quantification, are imperative if novel therapeutics that are based on blocking the transcription pathway are to be realized.

The functional domain of p300 that is responsible for acetylation of histone is the HAT domain, and the bromo domain, a conserved 110 amino acid structural motif, is thought to be responsible for binding to both unacetylated and acetylated histone,[8,9] where no preference of the isolated bromo domain toward either of the unacetylated and the acetylated histone was revealed in an *in vitro* ensemble study.[9] Although, a recent report by Delvecchio et al., on the crystal structure of catalytic core of CBP-p300 shows that the bromo, PHD (plant homeo domain), RING (really interesting new gene), and HAT domains adopt an assembled configuration and form a compact module,[10] clearly showing that the bromo domain is located proximal to the HAT domain, little information on the relative location of the HAT domain with respect to the structure of the full-length p300 (p300FL) is available so far.[11] Neither is there existing detail on the nature of interactions within the p300FL−histone complexes. Such paucity of information on p300FL could be related to the protein being too large, making NMR data interpretation complicated and/or crystallization difficulties due to the presence of unstructured regions within the protein fold.

Other than the histone proteins, p300 is known to acetylate High Mobility Group Box 1 or HMGB1, which is a ∼25 kDa chromosomal protein, found in abundance and highly conserved across species. Apart from functioning as a nuclear architectural protein, HMGB1 exhibits extracellular functions, related to inflammation and tumor growth.[12] During necrosis, HMGB1 can passively leak out from cells upon loss of integrity of the cell

Received: August 11, 2015
Revised: September 15, 2015
Published: September 29, 2015

DOI: 10.1021/acs.jpcb.5b07795
J. Phys. Chem. B 2015, 119, 13278−13287

membrane.[13] Extracellular HMGB1 is a reliable indicator of necrosis, and an immediate trigger for inflammation. In fact, the extracellular HMGB1 can be regarded as a "danger signal" that communicates death of the cell to its neighbors. Bonaldi et al. have provided a molecular level characterization of the mechanism of transfer of HMGB1 from nucleus to the secretory lysosomes.[14] They found out that HMGB1 shuttles actively between the nucleus and cytoplasm, and acetylation of HMGB1 triggers its accumulation in cytoplasm and then in the cytosol. Among the 43 lysine residues, over a total of 214 amino acids, they identified 17 acetylated lysines, which are responsible for shifting HMGB1 from nucleus to cytoplasm. Though it is recognized that acetylation of HMGB1 by p300/CBP plays a crucial role in shifting HMGB1 from nucleus to cytoplasm,[14] there is no report on the structural architecture of the complex between full-length p300 (p300FL) and HMGB1, neither is there any information available on the nature of interaction between the two proteins. Because release of HMGB1 by necrotic cells triggers inflammation, having pathological consequences in sepsis, arthritis, cancer, and other diseases, understanding the fundamental events behind the extracellular release of HMGB1 is important for identifying effective therapeutic routes. Inhibiting the acetylation event and thereby preventing HMGB1 accumulation within the extranuclear space could be one such avenue, for which deciphering the interactions within the p300FL−HMGB1 complex in quantifiable terms would be crucial.

Herein, atomic force microscopy (AFM), a high-resolution imaging method used for acquiring information on single biomolecules,[15] has been employed to obtain a contour map of the complexes between full-length p300 (p300FL) and histone/HMGB1 proteins. Previously, we acquired AFM-derived information[11] on the structural features of p300FL, e.g., gross shape, monomeric/multimeric state, plausible locations of the C- and N-terminals, and location of binding of the tumor suppressor p53 − one of the most important transcription factors whose function is initiated by site-specific recruitment of p300[16,17] and that plays a key role in transcriptional activation of genes involved in cell cycle arrest and apoptosis.[18] Indeed, p300 is known to interact with other transcription factors such as Jun, CREB, c-Myb, nuclear hormone receptors, and E2F, to name a few.[19]

In the past decade, various reports on complexation between different domains of p300, particularly the bromo domain, and histone have been made.[9,20,21] However, none of these offers information related to the full-length p300. Here, a biophysical approach has been adopted, and the interaction forces acting between p300FL and each of histone octamer (having two copies of each of H2A, H2B, H3, and H4), histone H3, which is thought to be the primary histone component directly participating in interaction with p300,[3,22] and HMGB1, have been probed using single molecule level atomic force spectroscopy (AFS). In recent times, AFS has emerged as a powerful tool for measuring intermolecular forces between different proteins[23,24] and within ligand−receptor pairs,[25,26] and for investigating the strength and kinetics of biomolecular complexes in near-native conditions.[27−29] In a typical AFS setup, meant for measuring the rupture/unbinding force, one protein is immobilized on the AFM probe and its counter protein is placed on the substrate surface. The AFM probe is brought toward the surface, allowing the proteins to bind, and is subsequently retracted, thereby inducing the rupture events to occur. By monitoring the approach−retraction cycle, the rupture force can be measured.[30,31] In this study, we have quantified the unbinding forces between p300FL and histone octamer/histone H3/HMGB1 and evaluated the off-rate constant, the length scale of potential barrier on the dissociation pathway, and the activation energy barrier values. Apart from delineating the energy landscape of the dissociation events, we have evaluated the effect of acetylation on the interaction forces by performing force measurement experiments in acetylating condition. We suggest that in absence of any information on the structure and stability of the complexes of p300FL with histone/HMGB1 proteins, the molecularly resolved AFM/AFS data could be significant.

MATERIALS AND METHODS

Full-Length p300 (p300FL) Purification and Solution Preparation. The methods for p300FL purification and solution preparation (see the Supporting Information for details) were similar to the methods described previously.[32]

Preparation of Histone Octamer, Histone H3, H3-Specific Antibody, and HMGB1 Solutions. Histone octamer, histone H3, H3-specific antibody and HMGB1 were purchased from Sigma-Aldrich. Stock histone octamer solution was prepared from lyophilized powder using 10 mM Tris−HCl [tris(hydroxymethyl)aminomethane hydrochloride] buffer (pH 7.5), 2 M NaCl, 1 mM EDTA, 5 mM 2-mercaptoethanol and further diluted, as required. Histone H3 was supplied in 8 mM PBS (phosphate-buffered saline) (pH 7.4), 110 mM NaCl, 2.2 mM KCl, 3 mM DTT (dithiothreitol), 20% glycerol. H3-specific antibody was supplied in 10 mM PBS. Stock H3-specific antibody solution was diluted to 20 μM for blocking experiment. Stock HMGB1 solution was supplied in 20 mM HEPES [4-(2-hydroxyethyl)-1-piperazineethanesulfonic acid] buffer (pH 7.8), 150 mM NaCl, 0.2 mM EDTA, 0.1% TRITON X-100, 2 mg/mL leupeptin, and 0.1 mM AEBSF [4-(2-aminoethyl)-benzenesulfonyl fluoride]. All the solutions were prepared immediately before the experiments.

Preparation of p300FL−Histone Octamer Complex. The p300FL (25 nM) and histone octamer (10 nM) solutions were taken in a binding buffer containing 10 mM HEPES (pH 7.6), 200 mM NaCl, 10 mM KCl, 1.5 mM $MgCl_2$, 10% glycerol, 0.05% NP-40 (nonylphenoxypolyethoxyethanol), 2 mM PMSF [(phenylmethyl)sulfonyl fluoride], 1 mM DTT and incubated at 4 °C for 2 h.[9]

Preparation of p300FL−p300 F-4 Complex. The complex formation method was kept similar to that of our previous work where a number of p300FL−antibody complexes were prepared.[11] Here the concentration of both the p300FL and p300 F-4 antibody was 10 nM.

Preparation of p300FL−HMGB1 Complex. The p300FL (10 nM) and the HMGB1 (10 nM) protein solutions were incubated in a buffer containing 50 mM Tris−HCl (pH 8.0), 10% glycerol, 1 mM DTT, 0.1 mM EDTA, 0.1 mM PMSF at 37 °C for 15 min.

Preparation of p300FL−HMGB1−anti HMGB1 Antibody Complex. The p300FL, HMGB1, and anti-HMGB1 antibody solutions (10 nM each) were mixed and incubated at 37 °C for 15 min to form the ternary complex.

AFM Sample Preparation for Imaging p300FL−Histone Octamer Complex in Air. The p300FL−histone octamer complex solution (2 μl) was deposited onto a freshly cleaved mica surface, kept for 15 min, then washed with 1 mL (500 μL × 2) HEPES binding buffer, followed by 1 mL (250 μL × 4) milli-Q ultrapure water (resistivity 18.2 MΩ cm), and dried under a gentle stream of nitrogen before imaging.

DOI: 10.1021/acs.jpcb.5b07795
J. Phys. Chem. B 2015, 119, 13278−13287

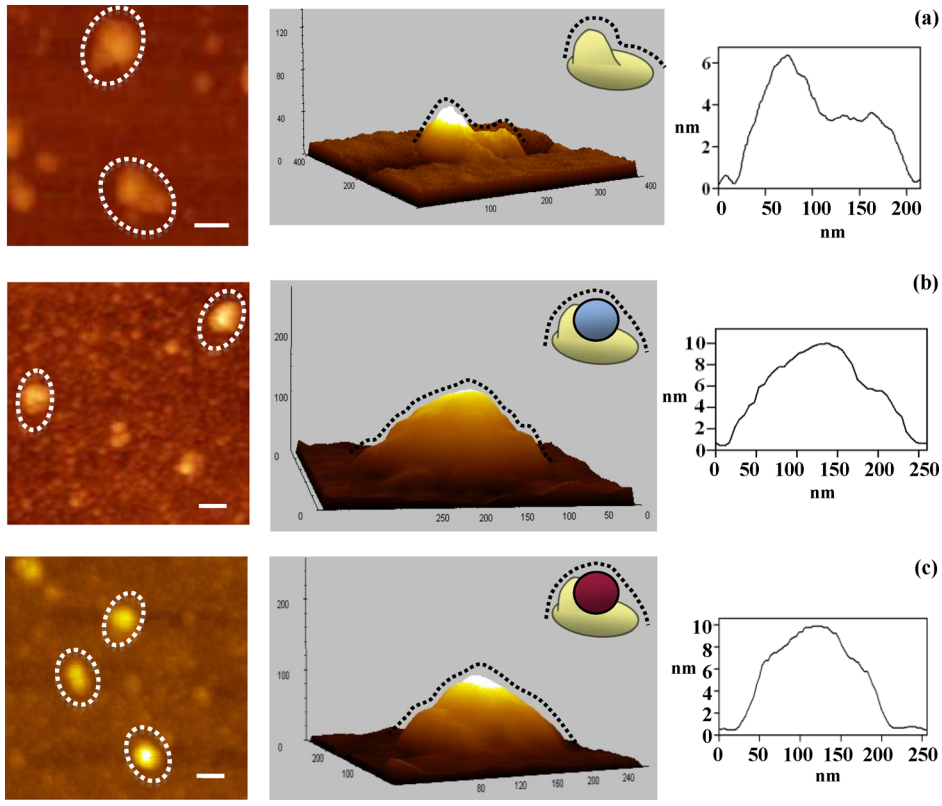

Figure 1. Representative top-view images, 3D views and the cross-section profiles of the (a) free p300FL, (b) p300FL–histone octamer complex, and (c) p300FL–p300 F-4 complex in ambient conditions. In the schematic drawings of the complexes, the blue ball indicates histone positioning and the maroon ball indicates positioning of p300 F-4 antibody on top of p300FL (yellow). The dotted lines over the contour of the complexes indicates the path of the AFM tip. For the 3D views, *x*, *y* axes are in nm and *z* axis is in Å. For the top views, scale bar 100 nm, *z* range 0–11 nm. The image shown in (a) is taken from ref 11.

AFM Sample Preparation for Imaging p300FL–Histone Octamer (or p300FL–HMGB1) Complex in Fluid. For fluid phase imaging of the complexes, gold(111) on mica substrate (Phasis, Switzerland) was modified with 3-mercaptopropionic acid (3-MPA), *N*-hydroxysuccinimide (NHS), and 1-ethyl-3-(3-(dimethylamino)propyl)carbodiimide (EDC), and the complexes were covalently immobilized. Imaging was always carried out using a freshly prepared sample in a buffered medium. See the Supporting Information for details.

AFM Probe Modification with p300FL. SNL-10 probe (Bruker) was cleaned in UV-ozone cleaner (Bioforce, Nanosciences) and silanized using 5% solution of (3-aminopropyl)-triethoxysilane (3-APTES) in 5% ethanol/95% water at room temperature (24 ± 1 °C) for 15 min. The tip was then rinsed with the 5% ethanol/95% water solution, followed by air-drying for 15–30 min. After that, the tip was immersed in a 2.5% glutaraldehyde solution in 100 mM Na-phosphate buffer (pH 7.0) for 45 min and then extensively rinsed with milli-q water. Then 20 nM p300FL solution was deposited on the tip and incubated for 30 min in normal ambient condition inside a sealed petridish. Finally, the probe was rinsed with the same buffer as used for preparing p300 solution and with milli-q water.[33] From the cantilever resonance frequencies measured before and after modification, a clear indication of material deposition could be obtained (Table S1). No change in resonance frequency after the force–distance cycle on histones indicates that the histone proteins were not picked up by the probe, and that the p300FL on AFM probe remained intact, after the complex rupture events took place (Table S1).

AFM Imaging and Force Measurement Data Acquisition and Analysis. AFM imaging was performed using a PicoLE AFM equipment (Agilent Corp., USA) with a 10 × 10 μm scanner at room temperature in the intermittent contact mode (acoustic alternating current mode). A standard rectangular silicon cantilever (μmasch, Estonia) was used for ambient imaging, and SNL-10 cantilevers (Bruker) were used for fluid imaging. See the Supporting Information for details.

Force measurement experiments were performed using the buffer composition same as that applied to carry out similar kinds of biochemical investigations reported earlier [10 mM HEPES (pH 7.6), 200 mM NaCl, 10 mM KCl, 1.5 mM $MgCl_2$, 10% glycerol, 0.05% NP-40, 2 mM PMSF, 1 mM DTT for histones;[9] and 50 mM Tris–HCl (pH 8.0), 10% glycerol, 1 mM DTT, 0.1 mM EDTA, 0.1 mM PMSF for HMGB1[14]]. For recording the force–distance curves, PicoView 1.12.2 software was used. The effective spring constants of the cantilevers were calibrated using in-built Thermal K software and were found to be 0.081–0.102 N/m. For the loading rate experiments, the retraction velocity of the cantilever was varied from 500 to 8000 nm/s. The effective loading rate (nN/s) was calculated by finding the slope (nN/nm) prior to the rupture event in the force–distance curve, and getting it multiplied by the retraction speed (nm/s) (assuming the retraction speed to remain constant during reproach). The kinetic parameters were determined using the effective loading rate. All the errors and error bars in force values are indicative of standard error of the mean. *P* values were calculated between different data sets of unbinding force values (see Table S2 in the Supporting Information) and significant differences indicated by

DOI: 10.1021/acs.jpcb.5b07795
J. Phys. Chem. B 2015, 119, 13278–13287

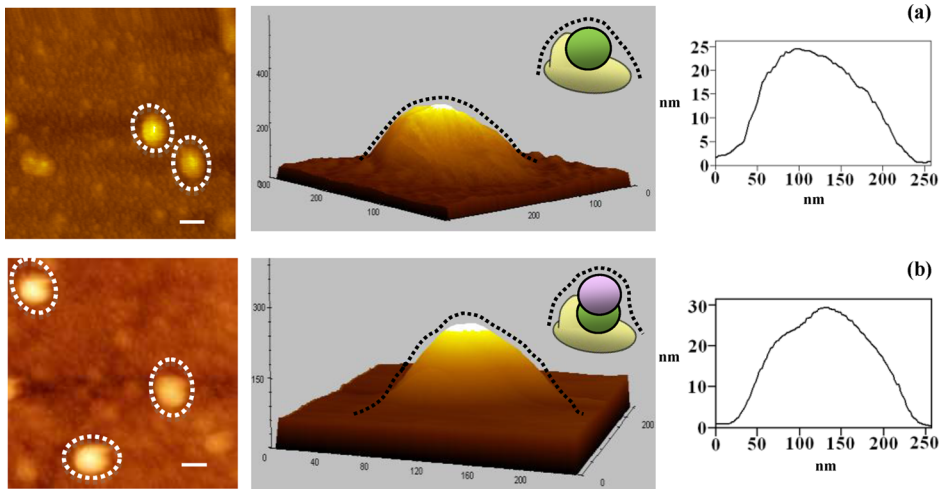

Figure 2. Representative the top-view images, 3D views and the cross-section profiles of the (a) p300FL−HMGB1 complex and (b) p300FL−HMGB1−anti-HMGB1 antibody complex in buffered medium. In the schematic drawing of the complexes, the green and the pink ball indicate the positioning of HMGB1 protein and anti-HMGB1 antibody, respectively. For the 3D views, *x*, *y* axes are in nm and *z* axis is in Å. For the top views, scale bar 100 nm, *z* range 0−30 nm.

$P < 0.0001$. See the Supporting Information for further details of force measurement experiments and data analysis.

RESULTS

In this work, the topographical contours of the p300FL−histone and the p300FL−HMGB1 complexes have been mapped by high-resolution AFM imaging, to distinguish the probable location of the p300FL HAT domain. Imaging was carried out in intermittent contact mode to minimize tip-induced damage of the soft protein exterior. To verify the location of the HAT domain of p300FL, a p300-specific antibody p300 F-4, which binds proximal to the p300FL bromo domain, was employed. The interaction forces operating between the histone proteins (histone octamer/histone H3) or HMGB1 (on substrate) and the p300FL (on AFM probe) were probed by force−distance curve analysis, in non-acetylating and acetylating conditions, and quantified by analyzing the retraction part of the force−distance curves. Dynamic force spectroscopy measurements were executed by changing the cantilever retraction speed, and specific kinetic parameters of the unbinding events were evaluated.

Topographic Features of p300FL−Histone Octamer and p300FL−HMGB1 Complexes. The high-resolution AFM images of free p300FL and its complex with histone octamer revealed an ellipsoidal shape of the molecule/complex (Figure 1a,b), where a distinct condense bulge, terminally positioned in free p300FL (Figure 1a), distinguished it from the complex having a centrally elevated contour (Figure 1b). The terminal bulge region is a characteristic feature of the free p300FL molecule and this region was earlier identified to be containing the N-terminal region of p300FL.[11] The average length along the long axis of the complex was found to be 156.1 ± 15.5 nm (ambient) and 148.2 ± 16.1 nm (fluid), and the height value of the complex was found to be 10.0 ± 2.0 nm (ambient), which is greater than that of free p300FL (6.4 ± 0.6 nm at terminal bulge region and 3.3 ± 0.1 nm at center), and is therefore compatible with histone binding. When histone molecules were separately characterized, most of the histone molecules were found to be near-spherical having a width value 24.0 ± 1.6 nm (7.2 ± 1.0 nm after tip-deconvolution, using equation $d_t = d_m^2/8r_{tip}$, where d_m is the measured diameter, d_t is the true diameter of the particle, and r_{tip} is the tip radius of curvature, which is 10 nm, as provided by the supplier,[34]) (data not shown). The tip-deconvoluted width of 7.2 nm is close to the histone octamer's crystallographic diameter of ∼6.5 nm,[35] indicating that most of the histone particles remained intact on surface. The height values of the complex and free p300FL in fluid were found to be 25.2 ± 2.0 and 19.5 ± 2.0 nm, respectively. The difference of about 6 nm conforms well to the tip-deconvoluted size (i.e., ∼7 nm) of a single histone octamer. Both the 3D view and the cross-section profile of the complex indicate that histone binding took place at a region just below the terminal bulge toward the central region of p300FL.

To confirm that histone binding occurs in the region of p300 containing the histone binding domains, we employed the p300-specific antibody p300 F-4 that binds proximal to the bromo domain, where histone protein is thought to bind.[9] A centrally protruded complex (Figure 1c) of average length 152.5 ± 12.5 nm and height 10.8 ± 2.0 nm was observed, the dimensions being quite similar to those of p300FL−histone octamer complex, plausibly because of the similar molecular weights of histone octamer (∼110 kDa) and p300-specific F-4 antibody (∼150 kDa) and a comparable binding stoichiometry of 1:1. From the contour of the complex, it is evident that the antibody binds at a region close to or same as the histone-binding region.

A centrally protruded complex contour could be observed also in the case of the p300FL−HMGB1 complex (Figure 2a). These complexes appeared to be ellipsoidal in shape and the average length was estimated to be 151.2 ± 14.0 nm. The terminal bulge region of p300FL containing the N-terminal of the protein[11] was no longer visible, indicating that the HMGB1 protein bound toward the central region of p300FL. The AFM height value was found to be 23.5 ± 1.5 nm, which is greater than that of the free p300FL (19.5 ± 2.0 nm), and is therefore indicative of binding of the HMGB1 protein.

Binding of HMGB1 at the central portion of p300FL was further verified by employing HMGB1 specific anti-HMGB1 antibody (Figure 2b). It was found that the p300FL−HMGB1−anti HMGB1 antibody complex was elongated in shape, having a centrally elevated contour, with a greater height value of 27.7 ± 1.2 nm than in the case of the p300FL−HMGB1 complex (Figure 2a). The contour and the increase in height value indicate binding of the antibody on top of the HMGB1 protein,

DOI: 10.1021/acs.jpcb.5b07795
J. Phys. Chem. B 2015, 119, 13278−13287

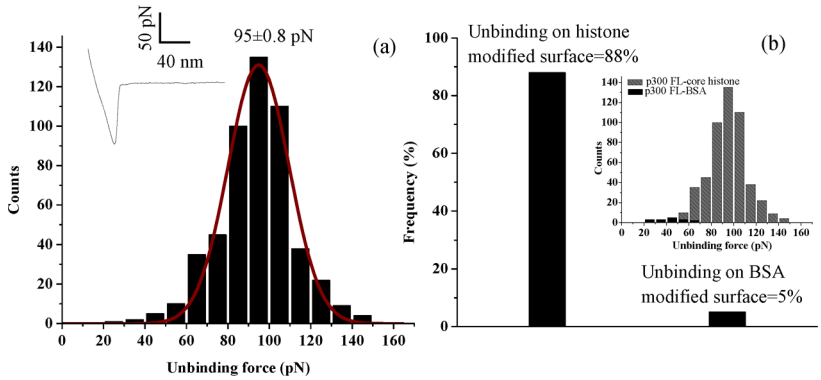

Figure 3. (a) Histogram of the unbinding force values for p300FL−histone octamer complex dissociation (from 516 force curves) and the representative force−distance curve (inset figure). The single peak distribution reveals a mean unbinding force of 95 ± 0.8 pN for loading rate 3 nN/s. (b) Unbinding frequency (i.e., the percentage of actual unbinding events with respect to the total number of attempts) between p300FL and the histone octamer modified surface, and the p300FL and BSA-modified surface. In the inset, histograms of force distribution on the histone octamer-modified surface (shaded bars) and BSA-modified surface (solid bars) are shown.

as shown in the schematic (Figure 2b), and confirms that HMGB1 binding region is situated at the central portion of p300FL.

It is to be noted here that p300FL being elongated/ellipsoidal in shape, tends to be adsorbed on the surface in a particular orientation. It has already been shown that at low concentration where the protein molecules are allowed to be adsorbed in a single isolated condition, the nonspherical proteins adsorb with their long axis parallel to the surface to release a greater number of solvent molecules and thereby increasing its translational entropy.[36,37] This has been the observation in our case too, where free p300FL has been visualized to be adsorbed reproducibly in a particular orientation generating repetitive features (the terminal big bulge protruded upward: 3D view in Figure 1a) in AFM topographs. The adsorption in a similar orientation of free p300FL and its complexes with different antibody molecules (his-tag mAb, IgG-AP, C-terminal and N-terminal specific antibody) has been shown in our previous work also.[11] The only other remaining possibility of adsorption of the complexes on the surface is unlikely because, in that situation, the p300FL molecule (300 kDa) is to be dangled above the comparatively smaller antibody molecules (150 kDa)/histone octamer (110 kDa). Hence, in the present situation, both the entropic and the spatial reasons trigger the adsorption of free p300FL/complexes in a particular orientation on the surface.

Measurement of Unbinding Force Required for p300FL−Histone Octamer Complex Dissociation. To obtain an idea about the intracomplex interactions, and to quantify the relevant unbinding force value, we performed single molecule level atomic force spectroscopy (AFS) experiments, taking p300FL on the AFM probe and histone proteins on the substrate surface. Dissociation of the histone octamers into smaller components during adsorption onto 3-MPA modified gold surface and subsequent washes, was checked by DLS experiments taking the washings. The first 1 mL washing revealed the presence of histone octamer, because a peak at a hydrodynamic diameter value of ∼9 nm, which could be attributed to the nonspecifically adsorbed histone octamers, was observed. The next two 1 mL washings did not show any indication of the presence of either octameric histone or any fragmented protein part because there was no particle distribution below ∼9 nm size. It indicates that the histone octamers remained intact on the surface, because, otherwise, the subsequent washes would have contained the protein fragments.

The essential control tests were performed prior to force measurement experiments. No adhesion peak could be observed in the control experiments (Figure S1), indicating occurrence of no rupture events, as the p300FL−histone octamer complexes were not formed in the first place. To verify whether the histone employed in our study was in octameric form or not, we carried out dynamic light scattering experiment (DLS) and calculated the hydrodynamic diameter of the protein in solution (Figure S2). This value was found to be 8.7 nm, which is close to the value (8.12 nm) reported for free histone octamer,[38] indicating that the histone used in this study was in octameric form.

The dissociation of the p300FL−histone octamer complex was typically characterized by a large adhesion peak (Figure 3a), from which the unbinding force could be evaluated. The most probable unbinding force value was determined from the peak of the distribution of independent rupture events and was found to be 95 ± 0.8 pN for the loading rate 3 nN/s (Figure 3a). The observation of a single peak distribution could imply dissociation of a single 1:1 complex during tip retraction,[23,39] because if the histogram contains more than one peak and if quantization of the force values appears, then it can be considered that more than one protein either on the surface or on the tip is involved in the unbinding event.[40,41] Measurements of the $f-d$ curves were reproducible over hours and typically for approximately 800−1000 approach−retract cycle. The unbinding force value as reported here is found to be in the range reported for other specific biological interactions studied at similar loading rates.[42,43]

To check for specificity of interaction between p300FL and histone octamer, the histone-modified surface was replaced with a BSA (bovine serum albumin)-coated surface where BSA molecules (10 nM) were immobilized onto the 3-MPA modified gold(111) surface and force−distance curves were recorded at different points. Almost no unbinding events were detected. Figure 3b shows a decrement in unbinding frequency from 88% to 5% upon replacing the histone-modified surface with the BSA-modified surface, indicating that the interaction between p300FL and the histone octamer, as exemplified in Figure 3a, was specific in nature. Histograms of force distribution for core histone and BSA-modified surface are shown in the inset of Figure 3b.

Measurement of the Unbinding Force Required for p300FL−Histone H3 Complex Dissociation. Because histone H3 is the component of histone octamer that exhibits preference toward p300 over the octameric histone,[9] AFS

DOI: 10.1021/acs.jpcb.5b07795
J. Phys. Chem. B 2015, 119, 13278−13287

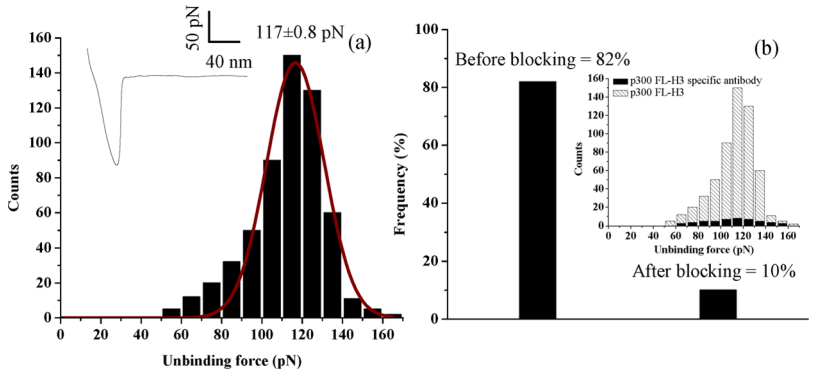

Figure 4. (a) Histogram of the unbinding force values for p300FL−histone H3 complex dissociation (from 567 force curves) and the representative force−distance curve (inset figure). A mean unbinding force of 117 ± 0.8 pN is elicited from the single peak distribution at loading rate 3 nN/s. (b) Unbinding frequency between p300FL and histone H3 before and after blocking with histone H3-specific antibody. In the inset, histograms of force distribution of p300FL−histone H3 (shaded bars) and in the presence of H3- specific antibody (solid bars) are shown.

analysis was performed by replacing the octamer with H3. A greater most probable unbinding force value of 117 ± 0.8 pN between p300FL and histone H3 (Figure 4a), compared to that for the p300FL−histone octamer complex, indicated stronger association of p300FL with H3, than with histone octamer, supporting the hypothesis of preferential binding of H3 to p300. The derived information presented here could also serve as control to the AFS data presented on histone octamer.

To verify if the measured forces were due to specific interactions between p300FL and histone H3, the H3 molecules on the surface were masked by addition of H3-specific antibody (20 μM), and force−distance curves were recorded with the same p300FL-modified tip, at different points on surface. Significant reduction in unbinding frequency from 82% to 10% took place (Figure 4b), indicating specificity of the p300FL−histone H3 complex formation event. A comparison between the force distributions before and after blocking is shown in the Figure 4b inset.

Evaluating the Kinetic Parameters for p300FL−Histone Complex Dissociation. To understand the dissociation mechanism of p300FL−histone octamer complex, the unbinding forces were plotted against the natural logarithm of loading rate ($\ln(r)$) (Figure 5). The dynamic force spectrum so obtained revealed a linear relationship between the unbinding force and the logarithm of loading rate. This indicates that the dissociation path has a single potential barrier in the energy landscape, resulting in a unique transition state of reaction.[44] The data were fitted with the Bell−Evans model[45,46] to determine the kinetic parameters of the unbinding process:

$$F = \frac{k_B T}{x_\beta} \ln\left(\frac{r x_\beta}{k_{off} k_B T}\right) \quad (1)$$

where F is the unbinding force, k_B is the Boltzmann constant, r is loading rate, T is absolute temperature, x_β is the length scale of potential barrier on the dissociation pathway, and k_{off} is the kinetic off-rate constant (at zero force). The x_β and k_{off} values at zero force condition were obtained by fitting the plot of F versus $\ln(r)$ with the above equation and relating to the slope and intercept of the linear fit, respectively. The slope $k_B T/x_\beta$ obtained by plotting F as a function of $\ln(r)$ resulted in $x_\beta = 0.183 \pm 0.01$ and 0.190 ± 0.01 nm for the p300FL−histone octamer and the p300FL−histone H3 complex, respectively. Extrapolation of the data to the loading rate at F = 0 allowed estimation of the dissociation rate constant ($k_{off} = r x_\beta / k_B T$) for the potential

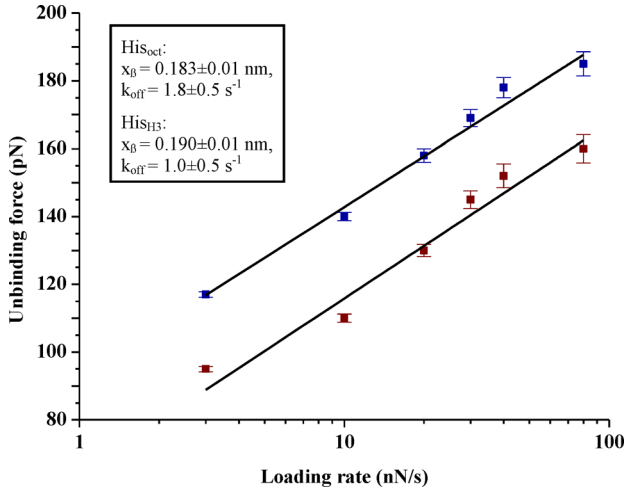

Figure 5. Dependence of the unbinding force between p300FL and histone octamer (His_{oct}) and histone H3 (His_{H3}) on the logarithm of loading rate. The maroon and the blue squares indicate data points for histone octamer and histone H3, respectively. The solid lines represent the numerical fit of the experimental data with Bell−Evans model. The obtained kinetic parameters are shown in the inset.

barrier, yielding $k_{off} = 1.8 \pm 0.5$ and 1.0 ± 0.5 s^{-1} in the case of the p300FL−histone octamer and the p300FL−histone H3 complex, respectively.

The activation energy barriers in the case of the p300FL−histone octamer and p300FL−histone H3 rupture events, $\Delta G^{\#}$, as estimated using the equation[47]

$$k_{off} = \frac{k_B T}{h} e^{-\Delta G^{\#}/k_B T} \quad (2)$$

where h is Planck's constant, were found to be 17.1 and 17.4 kcal/mol, respectively, correlating well with the respective k_{off} values. The lifetime of the p300FL−histone H3 complex at zero force defined as $1/k_{off}$[43] was found to be 1.0 s, nearly twice in comparison to 0.55 s as obtained in the case of the p300FL−histone octamer complex.

Evaluating the Unbinding Force and the Kinetic Parameters for p300FL−HMGB1 Complex. Prior to carrying out the force spectroscopy experiments on the p300FL−HMGB1 complex, the control tests, for example, recording the force−distance (f−d) curves between the APTES−glutaraldehyde modified tip and HMGB1-modified gold surface, and

DOI: 10.1021/acs.jpcb.5b07795
J. Phys. Chem. B 2015, 119, 13278−13287

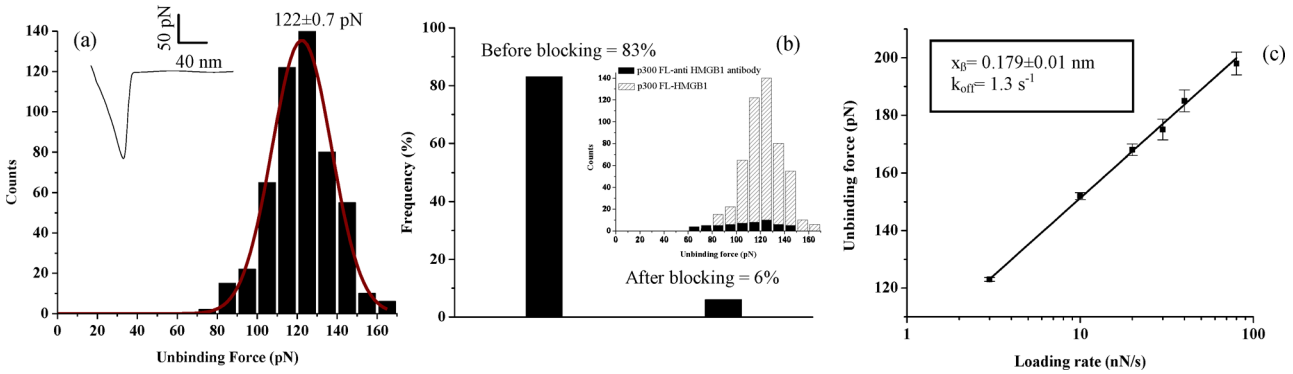

Figure 6. (a) Measurement of unbinding force for p300FL−HMGB1 complex dissociation from 517 force curves taken at loading rate 3 nN/s, and the representative force curve (shown in inset). From the single peak distribution, the mean unbinding force value of 122 ± 0.7 pN is elicited. (b) Unbinding frequency between p300FL and HMGB1 before and after blocking with HMGB1-specific antibody. In the inset, histograms of force distribution of p300FL−HMGB1 (shaded bars) and in the presence of anti- HMGB1 antibody (solid bars) are shown. (c) Dependence of the unbinding force values on the logarithm of loading rate, where the solid line represents the numerical fit of the experimental data with the Bell−Evans model. The obtained kinetic parameters are shown in the inset.

between the p300FL buffer-coated tip and HMGB1-modified gold surface, were routinely performed. No adhesion peak similar to that for the rupture of the p300FL−HMGB1 complex could be observed (Figure S3). The rupture events of the p300FL−HMGB1 complex were typically designated by a large adhesion peak and the most probable unbinding force value, which was determined from the peak of the force distribution, was found to be 122 ± 0.7 pN (Figure 6a). The single peak distribution of rupture forces indicates rupture of single p300FL−HMGB1 complex and excludes the statistically distributed simultaneous ruptures of several complexes. Measurements of the *f*−*d* curves were reproducible over hours and typically were for approximately 800−1000 approach−retract cycles. The specificity of interaction between p300FL and HMGB1 was checked by blocking the HMGB1 molecules with anti-HMGB1 antibody (20 μM). The unbinding frequency dropped drastically from 83% to 6% (Figure 6b), indicating that the interaction between p300FL and HMGB1 (Figure 6a) is specific in nature.

The dynamic force spectrum obtained, in the case of the p300FL−HMGB1 complex, revealed a linear relationship between the unbinding force and the natural logarithm of the loading rate (Figure 6c), indicating that a single potential barrier was present in the energy landscape, having a unique transition state of reaction. The data were fitted with the Bell−Evans model[45,46] (see eq 1), and the kinetic parameters, x_β and k_{off} at the zero force condition, were obtained by applying steps similar to those in the case of the p300FL−histone complexes. The x_β and the k_{off} values were estimated to be 0.179 ± 0.01 nm and 1.3 s^{-1}, respectively, and the lifetime of the complex was found to be 0.8 s.

Effect of Acetylating Medium on Unbinding Forces for p300FL−Histone Octamer, p300FL−Histone H3, and p300FL−HMGB1 Complexes. As the single molecule force spectroscopy measurements could delineate the interaction profiles for the p300FL−unacetylated histone octamer/histone H3/HMGB1 complexes, the reasonable step forward was to assess whether the interaction force values were affected in acetylating conditions (a medium relevant to the action of p300FL as HAT). The experimental setup was kept similar to that in the case of unacetylated histones, except for using an acetylating buffer [50 mM Tris−HCl (pH 8.0), 10% glycerol, 1 mM DTT, 1 mM PMSF, 10 mM sodium butyrate, 6 pM acetyl CoA[1]] inside the AFM fluid cell. The most probable unbinding force values, obtained from the peaks of the force distributions, were 66 ± 0.8 and 97 ± 0.7 pN for the p300FL−histone octamer and the p300FL−histone H3 complex, respectively (Figure 7). In the case of the p300FL−HMGB1 complex, the effect of acetylation was investigated using the acetylating medium, i.e., 50 mM Tris−HCl (pH 8.0), 10% glycerol, 1 mM DTT, 0.1 mM EDTA, 0.1 mM PMSF, 10 mM sodium butyrate, 18 mM acetyl CoA.[14] Under the acetylating condition, the unbinding force value was estimated to be 102 ± 0.8 pN (Figure 7), which is significantly less compared to the force value obtained in the case of the non-acetylating situation (Figure 6).

It is worthwhile to mention here that it would be oversimplified to assess the total extent of acetylation from the present type of experiment, because here the effects of acetylation of only the surface-exposed lysine residues that come in close proximity with p300FL during the force−distance cycle can be monitored. The present set of experiments tells us if there is a change in the interaction force due to acetylation in real time. This approach is unique in the sense that it allows us to retrieve local information at a given point of the entire course of acetylation reaction. It is tempting to propose that the present strategy permits one to identify the signature of single (or a few) acetylation event(s).

DISCUSSION

In the present study, molecularly resolved information related to the structure and dissociation kinetics of each of the complexes p300FL−histone octamer, p300FL−histone H3, and p300FL−HMGB1 have been elicited from the AFM-based single molecule force spectroscopy experiments. Two important facts could be derived from these information, which are discussed in the following sections.

Histone and HMGB1 Proteins Share a Common Binding Region of p300FL. The observation of a centrally elevated contour for both the complexes of p300FL with histone octamer (Figure 1b) and HMGB1 (Figure 2a), in which the terminal bulge as present in free p300FL contour (Figure 1a) has clearly disappeared, indicates a common binding region of p300FL, at a region just below the terminal bulge. Because histone (in both unacetylated and acetylated forms) is known to bind to the isolated bromo domain,[9] it is quite likely that the bromo domain is sited at this region of p300FL. Given that acetylation of histone proteins takes place via the action of HAT

DOI: 10.1021/acs.jpcb.5b07795
J. Phys. Chem. B 2015, 119, 13278−13287

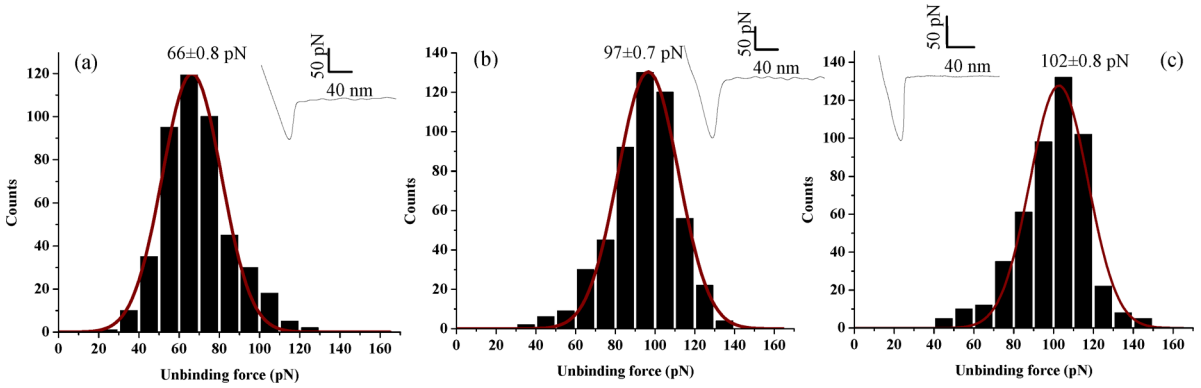

Figure 7. Measurement of unbinding force values in acetylating conditions for (a) the p300FL−histone octamer complex, (b) the p300FL−histone H3 complex, and (c) the p300FL−HMGB1 complex, from the histograms of 461 force curves (p300FL−histone octamer), 516 force curves (p300FL−histone H3), and 490 force curves (p300FL−HMGB1) obtained at loading rate 3 nN/s. The representative force−distance curves are shown in the respective insets. The single peak distributions reveal mean unbinding force values of 66 ± 0.8 pN (p300FL−histone octamer), 97 ± 0.7 pN (p300FL−histone H3), and 102 ± 0.8 pN (p300FL−HMGB1).

domain of p300FL,[2] it is reasonable to propose that the bromo domain and the HAT domain are proximally situated, and therefore, the HAT domain can also be located at or near the terminal bulge region of p300FL. A recent report by Delvecchio et al., on the crystal structure of the catalytic core of CBP-p300 has revealed that the bromo, PHD, RING, and HAT domains adopt an assembled configuration and form a compact module,[10] clearly supporting the AFM-based prediction of proximal location of the bromo domain to the HAT domain. In one earlier study, it was indicated that the HAT domain, being the largest domain (residues 1284−1517) of p300FL, could be a part of the biggest bulge observed in the AFM image of p300FL.[11] Binding of histone octamer and HMGB1 at the junction between the bulge and the non-bulge region, of p300FL, is therefore justified, because for acetylation of histone and HMGB1, the protein should bind to a location near or at the HAT domain of p300FL, so that the binding message can be translated to the catalytic (HAT) domain of p300FL. Interestingly, it was found in a high-resolution AFM imaging study[11] that p53, the tumor-suppressor protein, also binds at the junction region between the bulge and the non-bulge regions of p300FL. A biophysical consequence of such a common binding region could be an obstruction set to the simultaneous binding of histone/HMGB1/p53 proteins to the p300FL, which could inhibit acetylation of these proteins.

p300FL Forms a Dynamic Complex with Each of Histone Octamer, Histone H3 and HMGB1 Protein. In the present study, the dynamic force measurements carried out using single molecule atomic force spectroscopy, allowed reconstruction of the energy landscape of dissociation events of the p300FL−histone/HMGB1 complexes, unattainable by any other techniques applied to these systems until now. In each of the three cases studied, i.e., p300FL−histone octamer, p300FL−histone H3, and p300FL−HMGB1 complex, the estimated k_{off} values are found to be similar to the k_{off} values characteristic of other ligand−receptor pairs, such as p53-Mdm2 pair (1.5 s^{-1}),[42] cadherins (1.8 s^{-1}),[48] selectins (2.8 s^{-1}),[49] etc. that are typical of low-affinity, dynamic interaction between two proteins rather than stronger complexes, e.g., antigen−antibody complexes that exhibit very low k_{off} values in the order of 10^{-10} s^{-1}. This is probably to be expected for a protein−protein complex, where one of the components is an enzyme molecule that would desire to leave after finishing its function as a catalyst.

The generally observed reduction in the unbinding force values under acetylating conditions (Figure 8), compared to the non-acetylating situation, could in fact be supportive to such transient binding as discussed above. In the case of the histone proteins, the decrease in the unbinding force value could be due to a change in the surface charge profile, as a result of acetylation of the positively charged surface lysine residues, and conversion of the amines of lysines to amides, effectively weakening interactions between p300FL and histone proteins. Importantly, the extent of reduction in unbinding force values, under acetylating condition, was found to be greater in the case of the p300FL−histone octamer complex (29 pN) than in the case of the p300FL−histone H3 complex (20 pN), which could be due to the presence of a greater number of surface-exposed lysine residues in histone octamer than in histone H3. In the case of HMGB1 too, a similar trend, i.e., reduction in the unbinding force upon acetylation (Figure 7), could have electrostatic component playing, because HMGB1 contains 43 lysine residues, some of which are densely located (three or four at a stretch) within the amino acid spans 28−44 and 179−185 that are known to be frequently acetylated.[50] The proposition of the presence of an electrostatic component in such interactions could be further justified, because the C-terminal of p300FL having acidic residues (aspartate and glutamate) was shown to reside at the junction between the bulge and the non-bulge region of the protein earlier.[11] In fact, the IBiD (interferon

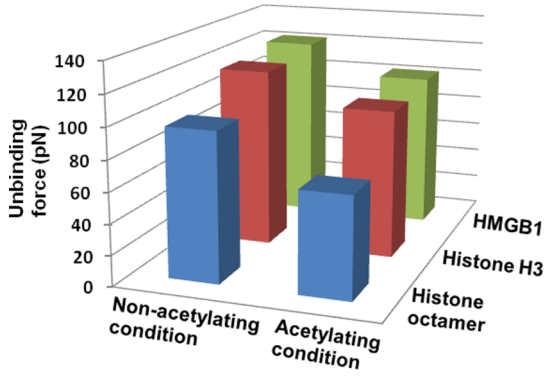

Figure 8. Comparative diagram for the unbinding force values for the three protein pairs (p300FL−histone octamer, p300FL−histone H3, and p300FL−HMGB1) in non-acetylating and acetylating condition.

DOI: 10.1021/acs.jpcb.5b07795
J. Phys. Chem. B 2015, 119, 13278−13287

response binding domain) domain, which is situated at the C-terminal region of p300FL, has a helical framework containing an apparently flexible polyglutamine loop that participates in ligand binding.[51] Indeed, acetylation-induced conformational change(s) of the histone/HMGB1 proteins could also be instrumental in weakening interactions with p300FL upon occurrence of the acetylation event. However, any such conformational change(s) need to be monitored and be thoroughly investigated before the origin of transient binding of p300FL to the histone/HMGB1 proteins can be established.

CONCLUSIONS

In conclusion, we have presented direct molecularly resolved AFM-based structural and kinetic information on binding/unbinding of the histone acetyltransferase (HAT) p300 (full-length), to the key nuclear proteins histone and HMGB1. The strength of the single molecule level monitoring of protein−protein interaction events by high-resolution AFM has been endorsed in the setting of the actions of important contributors of chromatin remodelling process. The observation of stronger binding of the histone H3 component, compared to the histone octamer, was elicited in both acetylating and non-acetylating conditions, indicating preferential binding of p300FL to histone H3, which is in agreement with the previously acquired biochemical information. Conversely, it was revealed that a change in the interaction force between p300FL and histone octamer/histone H3 occurred when the histone proteins were acetylated—information that was not available from the previous biochemical observations, most likely because the biochemical measurements were performed using the bromo domain, and not the full-length p300, where involvement of domain(s) other than the bromo domain cannot be ruled out. The AFM-based single molecule level analysis allowed us to delineate the energy landscape of the dissociation event and, therefore, provided a more detailed view of the dissociation events in general, compared to the ensemble studies, revealing that p300FL forms a dynamic complex with histone and HMGB1 proteins.

ASSOCIATED CONTENT

Supporting Information

The Supporting Information is available free of charge on the ACS Publications website at DOI: 10.1021/acs.jpcb.5b07795.

Tables of changes in resonance frequency of the cantilever after different modification steps and of different force values measured in acetylating and non-acetylating conditions with their respective error, sample size, and *P* values, purification and preparation methods, experimental details for AFM sample preparation, data acquisition and analysis, and for DLS experiments, and figures of force−distance curves, hydrodynamic diameter distributions (PDF)

AUTHOR INFORMATION

Corresponding Author

*E-mail: bcrm@iacs.res.in. Telephone: 0091-33-2473 4971 (Extn. 1506).

Present Address

‡School of Medicine, Case Western Reserve University, Cleveland, Ohio, USA.

Notes

The authors declare no competing financial interest.

ACKNOWLEDGMENTS

R.M. acknowledges financial support from IACS, Kolkata and CSIR, Govt. of India [Grant no. 01(2775)/14/EMR-II] and from DST, Govt. of India [Grant no. SB/SO/BB-33/2014]; the research fellowships of S.B., S.S., and T.R. from CSIR, Govt. of India and IACS, Kolkata, respectively; and Professor Tapas Kundu of JNCASR, Bangalore, and Professor Siddhartha Roy of IICB, Kolkata, for discussions and help with p300FL and p300 F-4.

REFERENCES

(1) Ogryzko, V. V.; Schiltz, R. L.; Russanova, V.; Howard, B. H.; Nakatani, Y. The transcriptional coactivators p300 and CBP are histone acetyltransferases. *Cell* **1996**, *87*, 953−959.

(2) Bannister, A. J.; Kouzarides, T. The CBP co-activator is a histone acetyltransferase. *Nature* **1996**, *384*, 641−643.

(3) Luebben, W. R.; Sharma, N.; Nyborg, J. K. Nucleosome eviction and activated transcription require p300 acetylation of histone H3 lysine 14. *Proc. Natl. Acad. Sci. U. S. A.* **2010**, *107*, 19254−19259.

(4) Schiltz, R. L.; Mizzen, C. A.; Vassilev, A.; Cook, R. G.; Allis, C. D.; Nakatani, Y. *J.* Overlapping but distinct patterns of histone acetylation by the human coactivators p300 and PCAF within nucleosomal substrates. *J. Biol. Chem.* **1999**, *274*, 1189−1192.

(5) Das, C.; Lucia, M. S.; Hansen, K. C.; Tyler, J. K. CBP/p300-mediated acetylation of histone H3 on lysine 56. *Nature* **2009**, *459*, 113−117.

(6) Hong, L.; Schroth, G. P.; Matthew, H. R.; Yau, P.; Bradbury, E. M. Studies of the DNA binding properties of histone H4 amino terminus. Thermal denaturation studies reveal that acetylation markedly reduces the binding constant of the H4 "tail" to DNA. *J. Biol. Chem.* **1993**, *268*, 305−314.

(7) Norton, V. G.; Imai, B. S.; Yau, P.; Bradbury, E. M. Histone acetylation reduces nucleosome core particle linking number change. *Cell* **1989**, *57*, 449−457.

(8) Chen, J.; Ghazawi, F. M.; Li, Q. Interplay of bromodomain and histone acetylation in the regulation of p300-dependent genes. *Epigenetics* **2010**, *5*, 509−515.

(9) Manning, E. T.; Ikehara, T.; Ito, T.; Kadonaga, J. T.; Kraus, W. L. p300 forms a stable, template-committed complex with chromatin: role for the bromodomain. *Mol. Cell. Biol.* **2001**, *21* (12), 3876−3887.

(10) Delvecchio, M.; Gaucher, J.; Gurrieri, C. A.; Ortega, E.; Panne, D. Structure of the p300 catalytic core and implications for chromatin targeting and HAT regulation. *Nat. Struct. Mol. Biol.* **2013**, *20*, 1040−1046.

(11) Banerjee, S.; Arif, M.; Rakshit, T.; Roy, N. S.; Kundu, T. K.; Roy, S.; Mukhopadhyay, R. Structural features of human histone acetyltransferase p300 and its complex with p53. *FEBS Lett.* **2012**, *586*, 3793−3798.

(12) Muller, S.; Scaffidi, P.; Degryse, B.; Bonaldi, T.; Ronfani, L.; Agresti, A.; Beltrame, M.; Bianchi, M. E. New EMBO members' review: the double life of HMGB1 chromatin protein: architectural factor and extracellular signal. *EMBO J.* **2001**, *20*, 4337−4340.

(13) Scaffdi, P.; Misteli, T.; Bianchi, M. E. Release of chromatin protein HMGB1 by necrotic cells triggers inflammation. *Nature* **2002**, *418*, 191−195.

(14) Bonaldi, T.; Talamo, F.; Scaffidi, P.; Ferrera, D.; Porto, A.; Bachi, A.; Rubartelli, A.; Agresti, A.; Bianchi, M. E. Monocytic cells hyperacetylate chromatin protein HMGB1 to redirect it towards secretion. *EMBO J.* **2003**, *22*, 5551−5560.

(15) Müller, D. J.; Dufrêne, Y. F. Atomic force microscopy as a multifunctional molecular toolbox in nanobiotechnology. *Nat. Nanotechnol.* **2008**, *3*, 261−269.

(16) Barlev, N. A.; Liu, L.; Chehab, N. H.; Mansfield, K.; Harris, K. G.; Halazonetis, T. D.; Berger, S. L. Acetylation of p53 activates transcription through recruitment of coactivators/histone acetyltransferases. *Mol. Cell* **2001**, *8*, 1243−1254.

DOI: 10.1021/acs.jpcb.5b07795
J. Phys. Chem. B 2015, 119, 13278−13287

(17) Liu, G.; Xia, T.; Chen, X. The Activation Domains, the Proline-rich Domain, and the C-terminal Basic Domain in p53 Are Necessary for Acetylation of Histones on the Proximal p21 Promoter and Interaction with p300/CREB-binding Protein. *J. Biol. Chem.* **2003**, *278*, 17557−17565.
(18) Das, S.; Boswell, S. A.; Aaronson, S. A.; Lee, S. W. P53 promoter selection: choosing between life and death. *Cell Cycle* **2008**, *7*, 154−157.
(19) Shiama, N. The p300/CBP family: integrating signals with transcription factors and chromatin. *Trends Cell Biol.* **1997**, *7*, 230−236.
(20) Ragvin, A.; Valvatne, H.; Erdal, S.; Arskog, V.; Tufteland, K. R.; Breen, K.; Øyan, A. M.; Eberharter, A.; Gibson, T. J.; Becker, P. B.; Aasland, R. Nucleosome binding by the bromodomain and PHD finger of the transcriptional cofactor p300. *J. Mol. Biol.* **2004**, *337*, 773−788.
(21) Winston, F.; David Allis, C. The bromodomain: a chromatin-targeting module? *Nat. Struct. Biol.* **1999**, *6*, 601−604.
(22) An, W.; Roeder, R. G. Direct Association of p300 with Unmodified H3 and H4 N Termini Modulates p300-dependent Acetylation and Transcription of Nucleosomal Templates. *J. Biol. Chem.* **2003**, *278*, 1504−1510.
(23) Taranta, M.; Bizzarri, A. R.; Cannistraro, S. Probing the interaction between p53 and the bacterial protein azurin by single molecule force spectroscopy. *J. Mol. Recognit.* **2008**, *21*, 63−70.
(24) Kim, H.; Lee, H. Y.; Lee, H. D.; Jung, Y. J.; Tendler, S. J. B.; Williams, P. M.; Allen, S.; Ryu, S. H.; Park, J. W. Interactions between Signal-Transducing Proteins Measured by Atomic Force Microscopy. *Anal. Chem.* **2009**, *81*, 3276−3284.
(25) Bartels, F. W.; Baumgarth, B.; Anselmetti, D.; Ros, R.; Becker, A. Specific binding of the regulatory protein ExpG to promoter regions of the galactoglucan biosynthesis gene cluster of Sinorhizobium meliloti–a combined molecular biology and force spectroscopy investigation. *J. Struct. Biol.* **2003**, *143*, 145−152.
(26) Kienberger, F.; Kada, G.; Gruber, H. G.; Pastushenko, V. Ph.; Riener, C.; Trieb, M.; Knaus, H. G.; Schindler, H.; Hinterdorfer, P. Recognition force spectroscopy studies of the NTA-His6 bond. *Single Mol.* **2000**, *1*, 59−65.
(27) Bonanni, B.; Kamruzzahan, A. S. M.; Bizzarri, A. R.; Rankl, C.; Gruber, H. G.; Hinterdorfer, P.; Cannistraro, S. Single molecule recognition between cytochrome C 551 and gold-immobilized azurin by force spectroscopy. *Biophys. J.* **2005**, *89*, 2783−2791.
(28) Hinterdorfer, P.; Dufrêne, Y. F. Detection and localization of single molecular recognition events using atomic force microscopy. *Nat. Methods* **2006**, *3*, 347−355.
(29) Sulchek, T.; Friddle, R. W.; Noy, A. Strength of Multiple Parallel Biological Bonds. *Biophys. J.* **2006**, *90*, 4686−4691.
(30) Rief, M.; Gautel, M.; Oesterhelt, F.; Fernandez, J. M.; Gaub, H. E. Reversible unfolding of individual titin immunoglobulin domains by AFM. *Science* **1997**, *276*, 1109−1112.
(31) Hinterdorfer, P.; Baumgartner, W.; Gruber, H. J.; Schilcher, K. Detection and localization of individual antibody-antigen recognition events by atomic force microscopy. H. *Proc. Natl. Acad. Sci. U. S. A.* **1996**, *93*, 3477−3481.
(32) Kar, S.; Sakaguchi, K.; Shimohigashi, Y.; Samaddar, S.; Banerjee, R.; Basu, G.; Swaminathan, V.; Kundu, T. K.; Roy, S. Effect of Phosphorylation on the Structure and Fold of Transactivation Domain of p53. *J. Biol. Chem.* **2002**, *277*, 15579−15585.
(33) Vinckier, A.; Gervasoni, P.; Zaugg, F.; Ziegler, U.; Lindner, P.; Groscurth, P.; Pluckthun, A.; Semenza, G. Atomic force microscopy detects changes in the interaction forces between GroEL and substrate proteins. *Biophys. J.* **1998**, *74*, 3256−3263.
(34) Dong, Y.; Shannon, C. Heterogeneous immunosensing using antigen and antibody monolayers on gold surfaces with electrochemical and scanning probe detection. *Anal. Chem.* **2000**, *72*, 2371−2376.
(35) Arents, G.; Burlingame, R. W.; Wang, B. C.; Love, W. E.; Moudrianakis, E. N. The nucleosomal core histone octamer at 3.1 A resolution: a tripartite protein assembly and a left-handed superhelix. *Proc. Natl. Acad. Sci. U. S. A.* **1991**, *88*, 10148−10152.
(36) Ramsden, J. J. Puzzles and paradoxes in protein adsorption. *Chem. Soc. Rev.* **1995**, *24*, 73−78.
(37) Norde, W. Adsorption of proteins from solution at the solid-liquid interface. *Adv. Colloid Interface Sci.* **1986**, *25*, 267−340.
(38) Banerjee, A.; Majumder, P.; Sanyal, S.; Singh, J.; Jana, K.; Das, C.; Dasgupta, D. The DNA intercalators ethidium bromide and propidium iodide also bind to core histones. *FEBS Open Bio* **2014**, *4*, 251−259.
(39) Fritz, J.; Katopodis, A. G.; Kolbinger, F.; Anselmetti, D. Force-mediated kinetics of single P-selectinyligand complexes observed by atomic force microscopy. *Proc. Natl. Acad. Sci. U. S. A.* **1998**, *95*, 12283−12288.
(40) Willemsen, O. H.; Snel, M. M.; Cambi, A.; Greve, J.; Grooth, B. G.; De Figdor, C. G. Biomolecular interactions measured by atomic force microscopy. *Biophys. J.* **2000**, *79*, 3267−3281.
(41) Allen, S.; Chen, X.; Davies, J.; Davies, M. C.; Dawkes, A. C.; Edwards, J. C.; Roberts, C. J.; Sefton, J.; Tendler, S. J. B.; Williams, P. M. Detection of Antigen−Antibody Binding Events with the Atomic Force Microscope. *Biochemistry* **1997**, *36*, 7457−7463.
(42) Funari, G.; Domenici, F.; Nardinocchi, L.; Puca, R.; D'Orazi, G.; Bizzarri, A. T.; Cannistraro, S. Interaction of p53 with Mdm2 and azurin as studied by atomic force spectroscopy. *J. Mol. Recognit.* **2010**, *23*, 343−351.
(43) Zhang, X.; Wojcikiewicz, E.; Moy, V. T. Force spectroscopy of the leukocyte function-associated antigen-1/intercellular adhesion molecule-1 interaction. *Biophys. J.* **2002**, *83*, 2270−2279.
(44) Merkel, R.; Nassoy, P.; Leung, A.; Ritchie, K.; Evans, E. Energy landscapes of receptor-ligand bonds explored with dynamic force spectroscopy. *Nature* **1999**, *397*, 50−53.
(45) Bell, G. I. Models for the specific adhesion of cells to cells. *Science* **1978**, *200*, 618−627.
(46) Evans, E.; Ritchie, K. Dynamic strength of molecular adhesion bonds. *Biophys. J.* **1997**, *72*, 1541−1555.
(47) Tinoco, I., Jr.; Bustamante, C. The effect of force on thermodynamics and kinetics of single molecule reactions. *Biophys. Chem.* **2002**, *101−102*, 513−533.
(48) Baumgartner, W.; Hinterdorfer, P.; Ness, W.; Raab, A.; Vestweber, D.; Schindler, H.; Drenckhahn. Cadherin interaction probed by atomic force microscopy. *Proc. Natl. Acad. Sci. U. S. A.* **2000**, *97*, 4005−4010.
(49) Hanley, W.; McCarty, O.; Jadhav, S.; Tseng, Y.; Wirtz, D.; Konstantopoulos, K. Single Molecule Characterization of P-selectin/Ligand Binding. *J. Biol. Chem.* **2003**, *278*, 10556−10561.
(50) Lotze, M. T.; Tracey, K. J. High-mobility group box 1 protein (HMGB1): nuclear weapon in the immune arsenal. *Nat. Rev. Immunol.* **2005**, *5*, 331−342.
(51) Lin, C. H.; Hare, B. J.; Wagner, G.; Harrison, S. C.; Maniatis, T.; Fraenkel. A small domain of CBP/p300 binds diverse proteins: solution structure and functional studies. E. *Mol. Cell* **2001**, *8*, 581−590.

DOI: 10.1021/acs.jpcb.5b07795
J. Phys. Chem. B 2015, 119, 13278−13287